Site C0016[1]

Expedition 331 Scientists[2]

Chapter contents

Background and objectives

Integrated Ocean Drilling Program (IODP) Site C0016 is located at the North Big Chimney (NBC) Mound in the Iheya North field (see Figs. F3 and F7 in Expedition 331 Scientists, 2011a). The hydrothermal mound is ~20 m high and 6 m in diameter and hosts vigorous hydrothermal vents on top of the mound with temperatures as high as 311°C, as well as extensive diffuse fluids with temperatures as high as 100°C that exit from small cracks and flanges in the mound. Adjacent to the main vent and within 5 m of diffuse venting, a polychaete (*Paralvinella hessleri*) colonizes the surface of the mound. Decapods (*Shinkaia crosnieri*) are abundant around these colonies at the top of the mound, on its sidewalls, and at several points at its foot, wherever there are diffusing fluids. Surrounding the decapod colonies are colonies of vent mussels (*Bathymodiolus* spp.). Most of the mussel colonies are distributed along the lower sidewalls and at the foot of the mound. The NBC Mound also has colonies of a tubeworm (*Lamellibrachia* sp.) on its top, located close to the polychaete colonies.

Based on chimneys that have been sampled and characterized elsewhere, the interior of the NBC hydrothermal mound is expected to consist of massive metal sulfide and sulfate deposits. Dominant minerals are expected to be anhydrite and barite, which may have built the structure, with pyrite and sphalerite infilling cavities. Based on seafloor observations, we expect the mound to contain a network of narrow hydrothermal conduits developed in its interior and within the underlying seafloor.

Previous microbiological characterization of the NBC chimneys has demonstrated that thermophilic Archaea, such as members of *Thermococcales*, *Archaeoglobales*, and *Methanococcales*, and thermophilic to mesophilic Bacteria, such as members of *Aquificales* and ?-*Proteobacteria*, are dominant (Nakagawa et al., 2005; Takai et al., 2006; Takai and Nakamura, 2010). These results indicate that chemolithoautotrophic metabolisms dependent on H_2 and/or sulfide/sulfur dominate the microbial communities within the chimneys. It would be valuable to examine the extent to which these same compositional and functional communities live within the larger structure of the NBC hydrothermal mound.

The scientific objectives of Site C0016 are thus very simple: to test whether a functionally active, metabolically diverse subvent biosphere exists within the NBC Mound and to characterize the variability and segregation of microbial communities within the

[1]Expedition 331 Scientists, 2011. Site C0016. *In* Takai, K., Mottl, M.J., Nielsen, S.H., and the Expedition 331 Scientists, *Proc. IODP,* 331: Tokyo (Integrated Ocean Drilling Program Management International, Inc.). doi:10.2204/iodp.proc.331.106.2011
[2]Expedition 331 Scientists' addresses.

doi:10.2204/iodp.proc.331.106.2011

mound structure fed by a deeply sourced high-temperature fluid.

Operations

Arrival at Site C0016

After we finished casing and capping operations at Hole C0014G, the D/V *Chikyu* moved to Site C0016, the top of NBC Mound (Fig. **F1**). Preparations began on the evening of 25 September 2010 and continued overnight into 26 September. After a seafloor survey with the remotely operated vehicle (ROV) in the early hours of 26 September, we were ready to drill into the mound (Table **T1**).

Hole C0016A

The desired location for the mound top site was a slight depression tagged at 1010.5 m drilling depth below seafloor (DSF) on 26 September 2010. A cloudy flow was observed from the hole almost immediately upon entry. Coring continued to 18 meters below seafloor (mbsf), often obscured by the strong cloudy outflow from the hole. The drill string was often observed to deviate from vertical by as much as 10°.

When penetration depth was reached and it was time to exit the hole, the outer barrel broke after a couple of spikes in overpull—up to 250 kN at the time of breakage! The flow from the drill hole was very strong at this time and flashed briefly, suggesting intense phase separation as the hot fluid poured out of the hole. The bit, split ring housing, extension sub, outer sleeve of the full closure catcher, and stabilizer were lost in the hole. The lower part of the inner barrel was dropped outside the hole but was later recovered by the ROV.

Hole C0016A was, needless to say, abandoned, with no recovered core.

Hole C0016B

After abandoning Hole C0016A, the *Chikyu* moved to the foot of NBC Mound. On the evening of 26 September 2010, the third guide base was placed at the foot of the mound, and we left to core at Site C0017 for a few days.

On 30 September, we returned to Site C0016 and entered the guide base in the early afternoon. Hole C0016B was spudded, and the first core was cut with the Baker Hughes INTEQ (BHI) system using a conventional friction core catcher. Coring went well, but upon tripping the 9 m barrel back to the ship, we discovered a total of only 71 cm of core, consisting of short segments of hard rock.

The second core at Site C0016 was taken on 1 October using an 18 m BHI barrel, again with the conventional friction core catcher. This time only 31 cm of core was recovered, comprising three quite hard pieces of different and interesting lithologies. These pieces fell out of the barrel when jostled slightly on deck, suggesting that much more core probably fell out during the retrieval trip. We decided to try one last 18 m core and strongly recommended that the full-closure core catcher be used to avoid losing more core.

The third and final core was taken on 2 October (yet again using the friction core catcher) on another 18 m barrel. Core 331-C0016B-3L recovered 72 cm of core consisting mostly of loose rubble. A total depth of 45 mbsf was achieved in this hole before we ended coring operations and capped the guide base. Rather than casing this hole, a 3 m length of pipe was added to the corrosion cap to guide instruments into the hole.

The cap was set by ROV on the evening of 2 October. By the morning of 3 October, the *Chikyu* had retrieved all transponders and was headed toward anchor point near Nakugusuku Port, Okinawa, Japan. Expedition 331 operations had come to an end, and the expedition officially ended when we arrived at port on 4 October.

Lithostratigraphy

Of the two holes drilled at Site C0016, Hole C0016A failed to recover any core and Hole C0016B recovered only 2.095 m of core, over a drilled interval from 0 to 45 mbsf, corresponding to a recovery of 4.7%. Additionally, all material recovered from the site is either hydrothermal precipitate or strongly hydrothermally altered volcanic rock. It is therefore not sensible to attempt a discussion of lithostratigraphy for Site C0016. Readers are referred to **"Petrology"** for a detailed description of the hydrothermal and altered volcanic lithologies recovered from the site.

Petrology

Two holes were attempted at Site C0016, the NBC hydrothermal sulfide mound at Iheya North Knoll.

Hole C0016A was spudded without a guide base into the crest of the NBC Mound. The hole failed spectacularly (see **"Operations"**), with a broken drill pipe and the bit left in formation. No core was recovered. We did observe flashing due to phase separation in video images from the ROV, both in vents at the top of the mound within 2 m of the hole prior to drilling and also during drilling within the hole itself. These

observations make it extremely unlikely that the fluid forming the NBC Mound has undergone phase separation within the underlying substrate.

Hole C0016B was drilled with a guide base immediately at the foot of the NBC mound, 20 m west of Hole C0016A. It was cored over an interval of 0 to 45 mbsf, with a recovery of only 2.1 m (4.7%) of core. As a result of this poor recovery, it is not possible to provide a holistic description of the alteration and mineralization within the sequence drilled. Instead, we detail the material collected in each core and provide a hypothesis on the relationships among the samples.

Core 331-C0016B-1L (0–9 mbsf)

We recovered 79 cm of competent hard rock as Core 331-C0016B-1L. During drilling, the bit penetrated very rapidly to ~6 mbsf and then slowed dramatically. It is therefore likely that the upper portion of the hole consists of soft and/or unconsolidated material and that the material recovered is from 6–9 mbsf.

Massive and semimassive sulfide

Intervals 331-C0016-1L-1, 0–31 cm, and 1L-1, 34–64 cm, comprise hard black clastic-textured massive sulfide (Fig. F2). The two intervals are similar, with the upper described in drill core as comprising rounded 1–5 mm fragments of ~10% soft-clay altered volcanic rock and ~10% hard siliceous volcanic rock, cemented in a hard matrix of ~60% sphalerite, 15% pyrite, and quartz. Coarser grained (2–3 mm) sphalerite, pyrite, galena, and possible chalcopyrite are associated with a late anhydrite vein down one side of the section.

The second interval of massive sulfide, interval 331-C0016-1L-1, 34–64 cm, is similar to the upper interval, with less abundant altered clasts (5%) and scattered irregular 2–4 cm patches of pale clay with sugary anhydrite (interpreted as possible late void fill). Sulfide is more abundant in the lower interval and is visually estimated as ~85% of the total volume, with half of this being pyrite.

A 3 cm interval separates the massive sulfide units and consists of hard gray, strongly silicified material with its clastic texture almost obliterated by silicification and only 15% sphalerite and 10% pyrite (visually estimated) (Fig. F2). This interval is a discrete fragment within the core, so its relationship to the surrounding massive sulfide intervals, the true depth interval it represents, and to what degree it is representative of that interval cannot be determined with any degree of certainty.

A polished thin section was cut of the upper massive sulfide interval. The section is estimated to contain 40% sphalerite, 10% pyrite, 4% galena, 1% chalcopyrite, 20% muscovite/illite, and 15% quartz, a mineralogy which is broadly in agreement with both the visual description of the core and the interpretation of X-ray diffraction (XRD) results for the massive sulfide (Table T2). In the section, illite/muscovite-pyrite altered clasts of volcanic rock, typically ~5 mm in size, and fragments of quartz, typically 1–2 mm in size, are cemented in a crystalline matrix of quartz-muscovite-sulfide (pyrite-sphalerite-chalcopyrite-galena) and late coarsely crystalline anhydrite (Fig. F3A, F3B).

Consistent paragenesis is present for the sulfide and sulfate phases in the section. Early iron-poor sphalerite appears to be detrital in origin and typically occurs as 0.5 mm subhedral, slightly rounded crystals, which commonly exhibit chalcopyrite disease (a dusting of submicrometer-sized "blebs" of chalcopyrite in sphalerite). This first generation of sulfide is overgrown by the other sulfide phases present in the sample. Pyrite occurs as euhedral to subhedral grains, both as single crystals and as overgrowths, with galena, on early sphalerite and is itself replaced by and overgrown by chalcopyrite (Fig. F3C). A second generation of iron-poor sphalerite overgrows early sphalerite (Fig. F3D) and other sulfide phases and also forms colloform- and atoll-textured aggregates (Fig. F3E), implying crystallization into open space. The final phase of precipitation is represented by coarse 2–3 mm anhydrite crystals, which overgrow all other phases in the sample (Fig. F3F).

Silicifed volcanic rock

The bottommost 15 cm of Core 331-C0016-1L consists of hard gray strongly silicified volcanic rock with ~5% coarsely disseminated 1 mm pyrite and sphalerite throughout the body of the rock. Coarser 2–3 mm sulfide (pyrite-sphalerite-minor galena) is associated with a quartz-anhydrite-10% sulfide vein that runs from the top of the section to ~10 cm (Fig. F4). Fine 1–2 mm wide irregular anastomosing veinlets of quartz with 10% sulfide also cut the rock. Like the semimassive sulfide farther up the core, the silicified volcanic rock is a discrete piece of core, so its spatial relationship to the overlying sulfide interval cannot be determined.

A polished thin section of silicified volcanic rock contained an estimated 60% quartz, 25% muscovite/illite, 5% anhydrite, 5% sphalerite, 5% pyrite, and trace quantities of galena and chalcopyrite, a mineralogy which is broadly in agreement with both the visual description of the core and the interpretation

of XRD results for the massive sulfide (Table T2). The section shows intergrown quartz-muscovite/illite-pyrite and sphalerite (Fig. F5A, F5B), with late coarse anhydrite veining and open space fill (Fig. F5C). There is no visible evidence of volcanic fabric in the thin section.

The most abundant sulfides are 1 mm subhedral sphalerite and 0.1 mm euhedral pyrite. The disseminated and vein sulfides display similar paragenesis to that seen in the overlying massive sulfide (see above). Early sphalerite is locally overgrown by a second generation of sphalerite or pyrite and/or minor galena. Pyrite shows replacement by and overgrowths of chalcopyrite (Fig. F5D, F5E).

Core 331-C0016B-2L (9–27 mbsf)

A total recovery of 31 cm was recorded for Core 331-C0016B-2L, with three distinct lithologies represented by three discrete pieces of core (Fig. F6).

Silicified volcanic rock

The uppermost 7 cm of the core comprises hard gray strongly silicified volcanic rock with a faint remnant clastic texture. About 5% pyrite and trace sphalerite are disseminated as very fine crystals and scattered coarser 0.1 mm euhedra throughout the rock. This unit is similar to the bottommost 15 cm recovered in Core 331-C0016B-1L and has a similar mineralogy, with quartz, pyrite, sphalerite, and minor muscovite detected by XRD (Table T2).

Coarse anhydrite

Interval 331-C0016B-2L-CC, 7–19 cm, is composed of a snow white coarsely crystalline anhydrite aggregate composed of 1–2 cm tightly intergrown acicular crystals (Fig. F6). The crystals show rough alignment in part of the sample, but their orientation relative to the core is meaningless because of the uncertainty of the true orientation of the sample. Most of the material is sulfide-free, except for a dark vein of 1–2 mm euhedral sphalerite-minor pyrite that lies along one edge of the interval.

Quartz-clay altered volcaniclastic breccia

Interval 331-C0016B-2L-CC, 20–31 cm (19–20 cm is void space) is volcanic breccia containing subangular 2 mm to 3 cm (dominantly 5–10 mm) soft gray clay–altered and slightly harder white sugary silica-clay-anhydrite-altered volcanic clasts hosted in a dark hard siliceous matrix (Fig. F6). Fine-grained pyrite is disseminated throughout the matrix, averaging ~3%, although the distribution is uneven. The clasts are also unevenly pyritic, containing up to 5% fine-grained pyrite as disseminations and occasional vesicle fill. The edge of an anhydrite-sphalerite-pyrite-trace galena vein runs along the top of the fragment. The vein is clearly truncated by drilling and is up to 1 cm wide, as exposed.

This breccia is similar in texture and structure to the material recovered from below 26 mbsf at Site C0013, although unlike that material, Mg chlorite was not detected via XRD at Site C0016. The mineralogy of the rock by XRD is quartz, pyrite, anhydrite, and muscovite/illite.

Core 331-C0016B-3L (27–45 mbsf)

Quartz-chlorite altered volcanic rock

A total of 99.5 cm of material was recovered as Core 331-C0016B-3L. The entire core consists of dark green to gray quartz-chlorite-altered volcanic rock with abundant stockwork veining (see below). The groundmass of the rock exhibits faintly defined fragments as large as ~1 cm in diameter, which may be clasts or which may have been generated by hydraulic fracture and veining of the rock. Very fine grained pyrite is disseminated throughout the rock at trace levels. XRD analysis identified an assemblage of quartz, chlorite, and pyrite.

Two generations of veining are present in the rock (Fig. F7):

1. Earlier sugary quartz-chlorite-pyrite veins, 2–3 cm wide, form a network, including a dark diffuse fine-grained quartz-pyrite halo. Veins contain euhedral pyrite, as coarse as 5 mm, in their centers, associated with green chlorite and sugary quartz.
2. Later pyrite-anhydrite veins crosscut the quartz-chlorite-pyrite veins and lack halos. They are slightly to strongly vuggy and comprise very coarse pyrite crystals (plus possible chalcopyrite), as coarse as 0.5–1 cm, with a sharply defined selvedge of anhydrite. They vary from hairline (anhydrite only) to 1 cm in thickness.

In total, including the veins, the core contains ~5% sulfide.

Significance of the alteration and mineralization at Site C0016

The recovery of massive sphalerite-rich sulfides in Hole C0016B marks the first time that this type of material, which strongly resembles the “black ore” from the Kuroko deposits of Miocene age from the Green Tuff region of Japan (Sato, 1974), has been recovered from beneath an active hydrothermal system on the seafloor. The textures and relationships seen in thin section for the massive sulfide require that a significant proportion of the sulfide mineral-

ization occurred via subseafloor precipitation, with at least some sphalerite precipitating into void space in the rock. Additionally, the sulfide and sulfate paragenesis of the samples shows an evolving system, with early sphalerite mineralization overprinted by pyrite and then chalcopyrite, as temperature increases, before a second sphalerite mineralizing event, as temperatures cool, and a final seawater influx, indicated by late coarse anhydrite.

As far as can be ascertained from shipboard data, the underlying altered volcanic rocks at Site C0016 show a similar evolution to the massive sulfide. The silicified volcanic rock from Core 331-C0016-1L shows similar sulfide paragenesis, and in all cases, anhydrite is among the last phases precipitated during alteration.

With increasing depth at Site C0016, the relative abundance of pyrite increases with respect to sphalerite, both on a local scale within the massive sulfide in Core 331-C0016-1L and overall within the sequence. This variation is one that is seen in many volcanic-hosted massive sulfide (VHMS) mineral systems and is interpreted to be a function of increasing temperature with depth (Large, 1992). The predominance at Site C0016 of quartz-muscovite/illite alteration grading to quartz-chlorite alteration at depth is also consistent with the proximal quartz-white mica grading to chloritic alteration commonly recorded in the immediate footwall of ancient VHMS systems, including the Miocene Kuroko deposits of Japan (Date et al., 1983).

Geochemistry

Headspace gas analysis

Because most of the recovered core at Site C0016 was hard, solid rock, only a single sample was recovered for headspace analysis (from Section 331-C0016B-3L-1). This sample, from 37 mbsf, yielded a methane concentration (Tables **T3, T4**) estimated to be between 86 and 310 µM. This estimate used the water content measured on nearby hard rock, and so is likely to be revised downward once water content is determined on the actual material used for the headspace analysis.

A high concentration of hydrogen was observed in Section 331-C0016B-3L-1, which might be an artifact of hydrogen production caused by BHI rotary drilling into hard pyritic rock.

Sediment carbon, nitrogen, and sulfur composition

For the three samples investigated, calcium carbonate ($CaCO_3$) content calculated from inorganic carbon concentration is low, ranging from below detection (<0.001 wt%) to 0.055 wt% (Table **T5**). Total organic carbon is also low, ranging from 0.007 to 0.022 wt%. Total sulfur (TS) is high, ranging from 7.7 to 23.2 wt%. The shallowest sample (from Section 331-C0016B-1L-1), a massive black ore rich in sphalerite and pyrite, has a TS content of 21.2 wt%. The next deepest sample (331-C0016B-1L-CC) is a silicified volcanic rock with a low TS content of 7.7 wt%, likely reflecting a higher silica content and lower abundance of pyrite. The deepest sample (331-C0016B-2L-CC) is an anhydrite-sulfide vein with a high TS of 23.2 wt%.

Microbiology

Cultivation of thermophiles

Growth of *Thermococcales* (e.g., *Thermococcus*) at 80°C and *Aquificales* (e.g., *Persephonella*) and thermophilic *Epsilonproteobacteria* (e.g., *Nitratiruptor*) at 55°C was examined onboard for Section 331-C0016B 1L-1, which was a "Kuroko" type of massive sulfide deposit. It was predicted that indigenous (hyper)thermophilic microorganisms would most likely occur in the vein structures of the massive sulfide deposits. However, no growth of any kind of microorganisms was observed.

Contamination tests

Drilling mud that adhered to the outer surface of core from Hole C0016B was collected for perfluorocarbon tracer (PFT) testing (Table **T6**) as a positive control on PFT concentration in drill mud used. Two of these core surface mud samples yielded PFT concentrations of 1.08 and 1.34 ppm/g.

Mud water Samples C0016B-1LMW and 2LMW from the onboard mixing tank used for drilling operations in Hole C0016B had PFT concentrations of 1.43 and 0.09 ppm/g, respectively. The type of mud fluid in Sample C0016B-1LMW was the most commonly used during drilling operations (see Table **T8** in Expedition 331 Scientists, 2011b) and is regarded as the most representative sample.

Comparison of PFT concentrations in predrilling (1.43 ppm) and postdrilling (1.08 and 1.34 ppm) mud samples indicates that the PFT concentration was essentially preserved in the drilling mud from mixing through drilling to core recovery. This suggests that external contamination can be estimated by directly comparing the concentrations of PFT in the core sample with that of the mud fluid prepared onboard.

Physical properties

Physical property measurements were made at Site C0016 to nondestructively characterize lithological units and states of sediment consolidation. Cores collected from this site were all composed of hard rock. Because the core was collected in a 4 inch liner, the multisensor core logger for whole-round samples (MSCL-W) measurement of *P*-wave velocity was not conducted.

Density and porosity

Bulk density at Site C0016 was determined from both gamma ray attenuation (GRA) measurements on whole cores (with the MSCL-W) and moisture and density (MAD) measurements on discrete samples (see **"Physical properties"** in Expedition 331 Scientists, 2011b). A total of four discrete samples were analyzed for MAD from Hole C0016B. Wet bulk density ranges from 2.4 to 2.9 g/cm^3 (Fig. **F8**). As at previous sites, GRA-derived density is somewhat lower (~2.0 g/cm^3) and exhibits more scatter (Fig. **F8**). Bulk density near the seafloor (0.3 mbsf) is 2.8 g/cm^3. It decreases to 2.4 g/cm^3 at 9 mbsf and then increases again to 2.8–2.9 g/cm^3 at 27–28 mbsf. Grain density was calculated from discrete MAD measurements and ranges from ~2.8 to 3.0 g/cm^3 (Fig. **F8**). Porosity was calculated from MAD measurements (Fig. **F9**). The water content in these rocks is quite low, between 3% and 10%, except at 9 mbsf where the porosity is higher (22%)

Density and porosity results are consistent with the presence of silicified rocks.

Electrical resistivity (formation factor)

Formation factor was not measured at Site C0016 because the resistivity electrode could not penetrate the lithified core material.

Discrete *P*-wave velocity and anisotropy measurements

P-wave velocity and relative anisotropy were measured on two sample polyhedrons collected from near the bottom of Hole C0016B. *P*-wave velocities at 27–28 mbsf range from 4000 to 4900 m/s (Fig. **F10**).

Thermal conductivity

Thermal conductivity was measured on split cores using the half-space probe method. A total of four measurements were made from Hole C0016B. Values range from a low of ~4 W/(m·K) at 9 and 27.1 mbsf to high values of 7.4 and 10.2 W/(m·K) at 0.3 and 28 mbsf, respectively (Fig. **F11**). Thermal conductivity is loosely and inversely correlated with porosity. As porosity decreases, thermal conductivity increases as water is forced from void spaces, because the thermal conductivity of grains is greater than that of water.

MSCL-I and MSCL-C imaging

MSCL-derived core images and color analyses are presented in the visual core descriptions (VCDs).

MSCL-W derived electrical resistivity

MSCL-W-based resistivity data are sparse. At 1 mbsf resistivity ranges from 1 to ~50 Ωm; at ~27 mbsf the maximum resistivity is higher, ~110 Ωm. (Fig. **F12**).

References

Date, J., Watanabe, Y., and Saeki, Y., 1983. Zonal alteration around the Fukazawa Kuroko deposits, Akita Prefecture, northern Japan. *Econ. Geol. Monogr.,* 5:365–386.

Expedition 331 Scientists, 2011a. Expedition 331 summary. *In* Takai, K., Mottl, M.J., Nielsen, S.H., and the Expedition 331 Scientists, *Proc. IODP,* 331: Tokyo (Integrated Ocean Drilling Program Management International, Inc.). **doi:10.2204/iodp.proc.331.101.2011**

Expedition 331 Scientists, 2011b. Methods. *In* Takai, K., Mottl, M.J., Nielsen, S.H., and the Expedition 331 Scientists, *Proc. IODP,* 331: Tokyo (Integrated Ocean Drilling Program Management International, Inc.). **doi:10.2204/iodp.proc.331.102.2011**

Large, R.R., 1992. Australian volcanic-hosted massive sulfide deposits: features, styles, and genetic models. *Econ. Geol.,* 87(3):471–510. **doi:10.2113/gsecongeo.87.3.471**

Nakagawa, S., Takai, K., Inagaki, F., Chiba, H., Ishibashi, J., Kataoka, S., Hirayama, H., Nunoura, T., Horikoshi, K., and Sako, Y., 2005. Variability in microbial community and venting chemistry in a sediment-hosted backarc hydrothermal system: impacts of subseafloor phase-separation. *FEMS Microbiol. Ecol.,* 54(1):141–155. **doi:10.1016/j.femsec.2005.03.007**

Sato, Y., 1974. Distribution and geological setting of the Kuroko deposits. *Soc. Min. Geol. Jpn., Spec. Iss.*, 6:1–9.

Takai, K., Nakagawa, S., Reysenbach, A.-L., and Hoek, J., 2006. Microbial ecology of mid-ocean ridges and back-arc basins. *In* Christie, D.M., Fisher, C.R., Lee, S.M., and Givens, S. (Eds.), *Back-Arc Spreading Systems: Geological, Biological, Chemical, and Physical Interactions*. Geophys. Monogr., 166:185–213.

Takai, K., and Nakamura, K., 2010. Compositional, physiological and metabolic variability in microbial communities associated with geochemically diverse, deep-sea hydrothermal vent fluids. *In* Barton, L., Mendl, M., and Loy, A. (Eds.), *Geomicrobiology: Molecular and Environmental Perspective:* New York (Springer), 251–283. **doi:10.1007/978-90-481-9204-5_12**

Publication: 4 October 2011
MS 331-106

Figure F1. Bathymetric map, Site C0016.

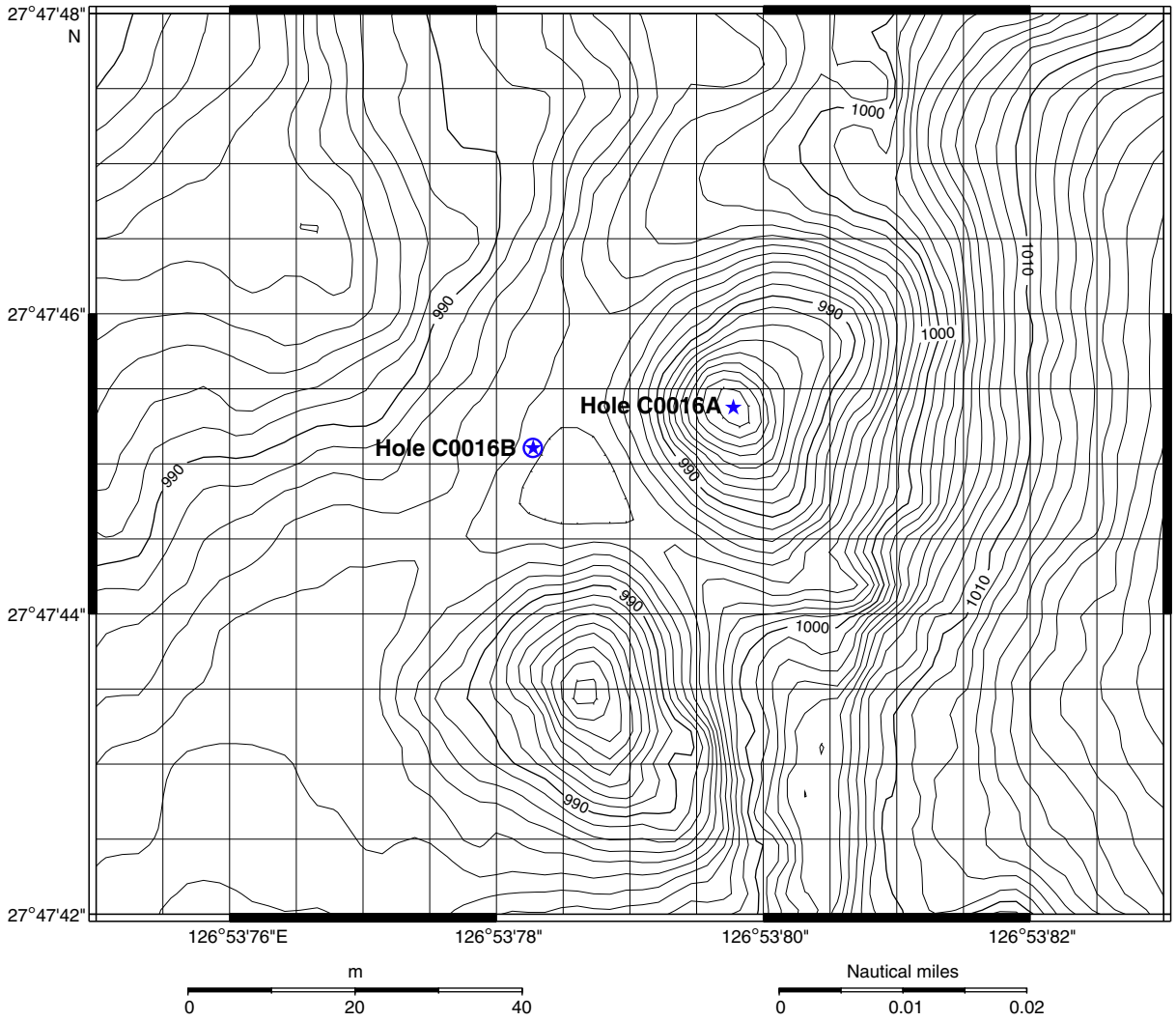

Figure F2. Core photograph showing massive and semimassive sulfide (interval 331-C0016B-1L-1, 0–63 cm).

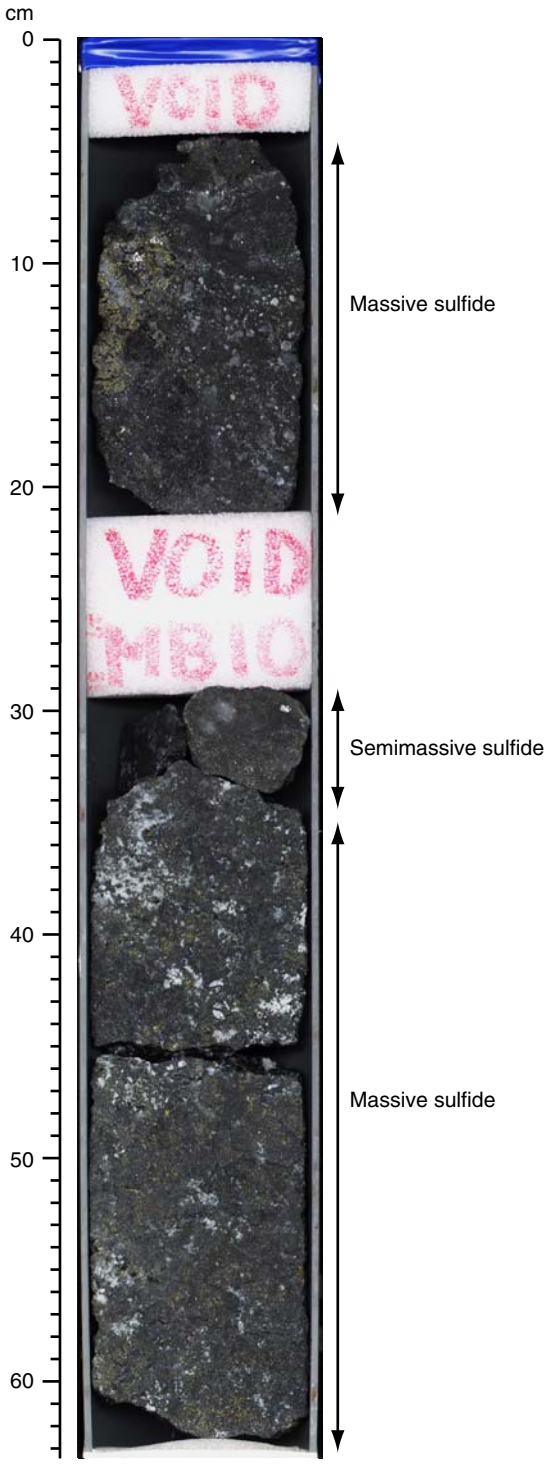

Figure F3. Photomicrographs of massive sulfide (Sample 331-C0016B-1L-1, 18–20 cm). **A.** Illite/muscovite-altered volcanic clast (indicated), containing disseminated pyrite and quartz fragments cemented in quartz-muscovite-sulfide (pyrite-sphalerite-chalcopyrite-galena) (plane-polarized light [PPL]; ×10). **B.** Same as A (reflected light [RL]; ×10). Sulfide phases are indicated. Py = pyrite, Cp = chalcopyrite, Sp = sphalerite, Gn = galena. **C.** Pyrite-chalcopyrite-sphalerite-galena intergrowth (RL; ×20). Chalcopyrite overgrows pyrite, and sphalerite shows chalcopyrite disease. **D.** Early subhedral sphalerite with a later overgrowth of sphalerite (PPL; ×5). **E.** Colloform/atoll-textured sphalerite overgrowing pyrite and chalcopyrite (RL; ×5). **F.** Coarse anhydrite overgrowing quartz and sulfide (PPL; ×2.5).

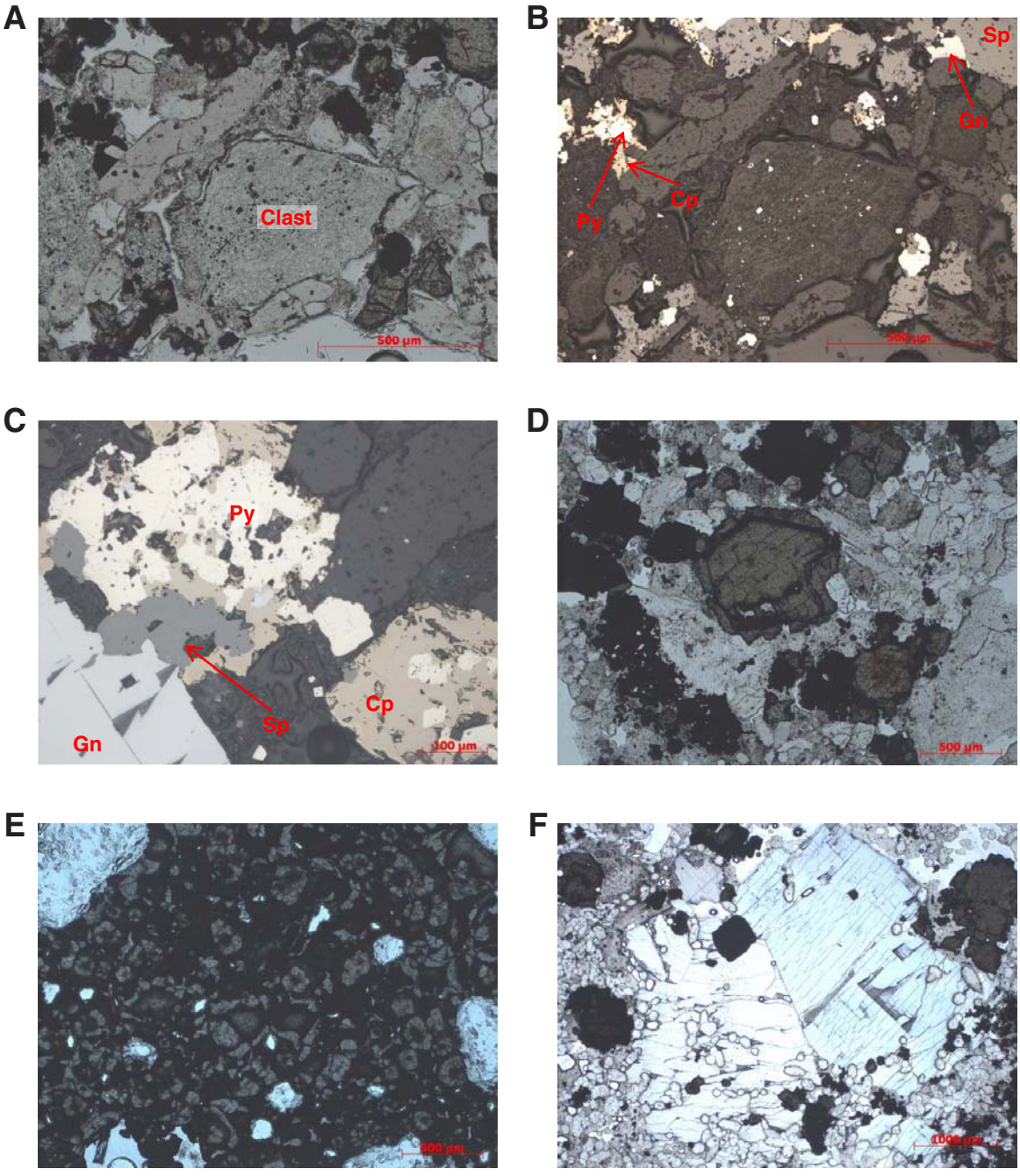

Figure F4. Core photograph showing silicified volcanic rock (interval 331-C0016B-1L-CC, 0–15 cm).

Figure F5. Photomicrographs of silicified volcanic rock (Sample 331-C0016B-1L-CC, 12–14 cm). Sulfide phases are indicated. Py = pyrite, Sp = sphalerite, Cp = chalcopyrite, Gn = galena. **A.** Representative view of sample. Intergrown quartz-muscovite/illite-sphalerite-pyrite (plane-polarized light [PPL]; ×5). **B.** Same as A (reflected light [RL]; ×5). **C.** Coarse anhydrite crystal (blue interference colors) overgrowing quartz, muscovite/illite, and sulfides (cross-polarized light; ×5). **D.** Sphalerite overgrown by galena, which is overgrown by pyrite, which is overgrown by chalcopyrite (RL; ×10). **E.** Higher magnification view of the galena-pyrite-chalcopyrite overgrowth boxed in D (RL; ×40).

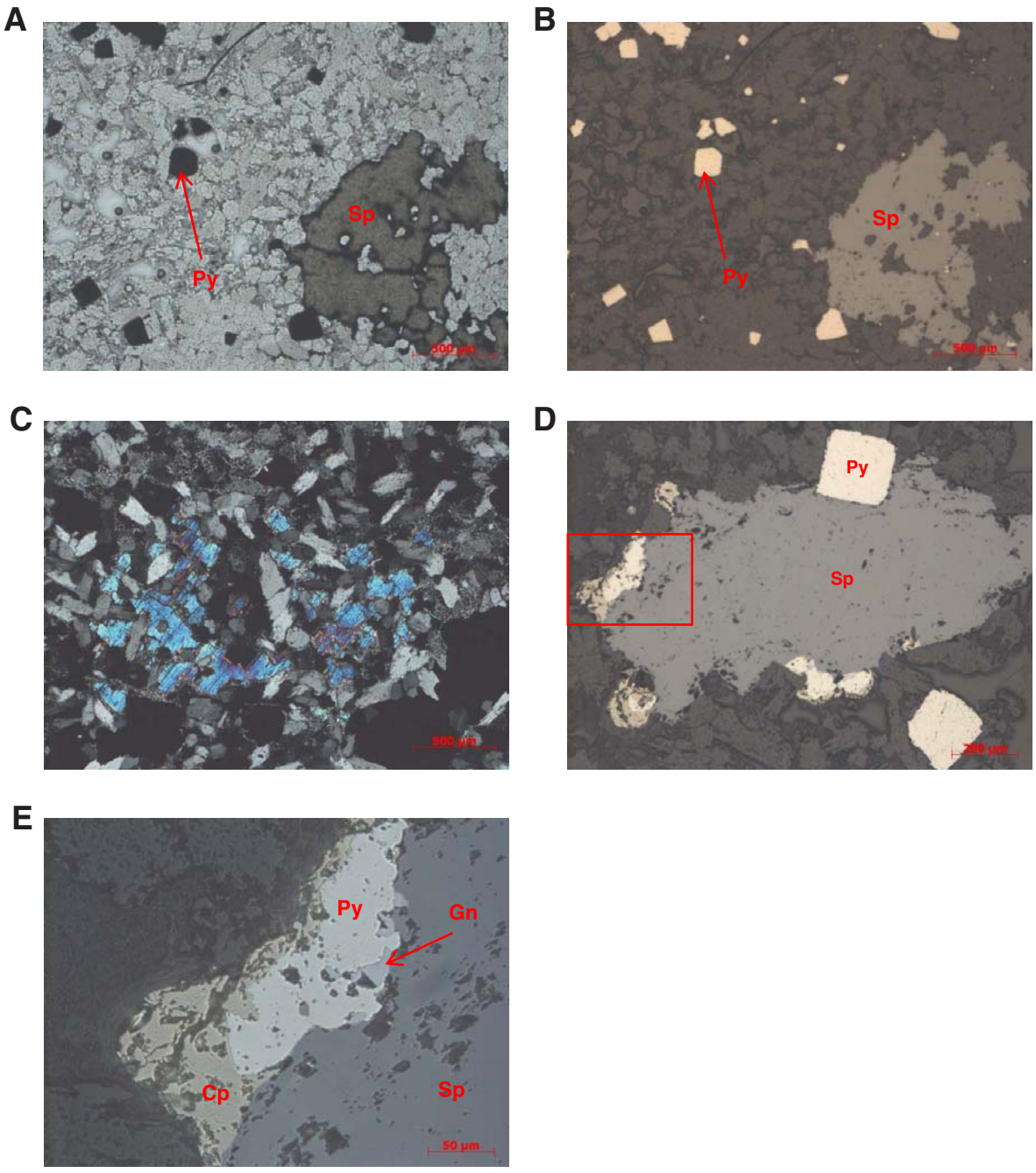

Figure F6. Core photograph showing lithologies recovered from interval 331-C0016B-2L-CC, 0–30 cm.

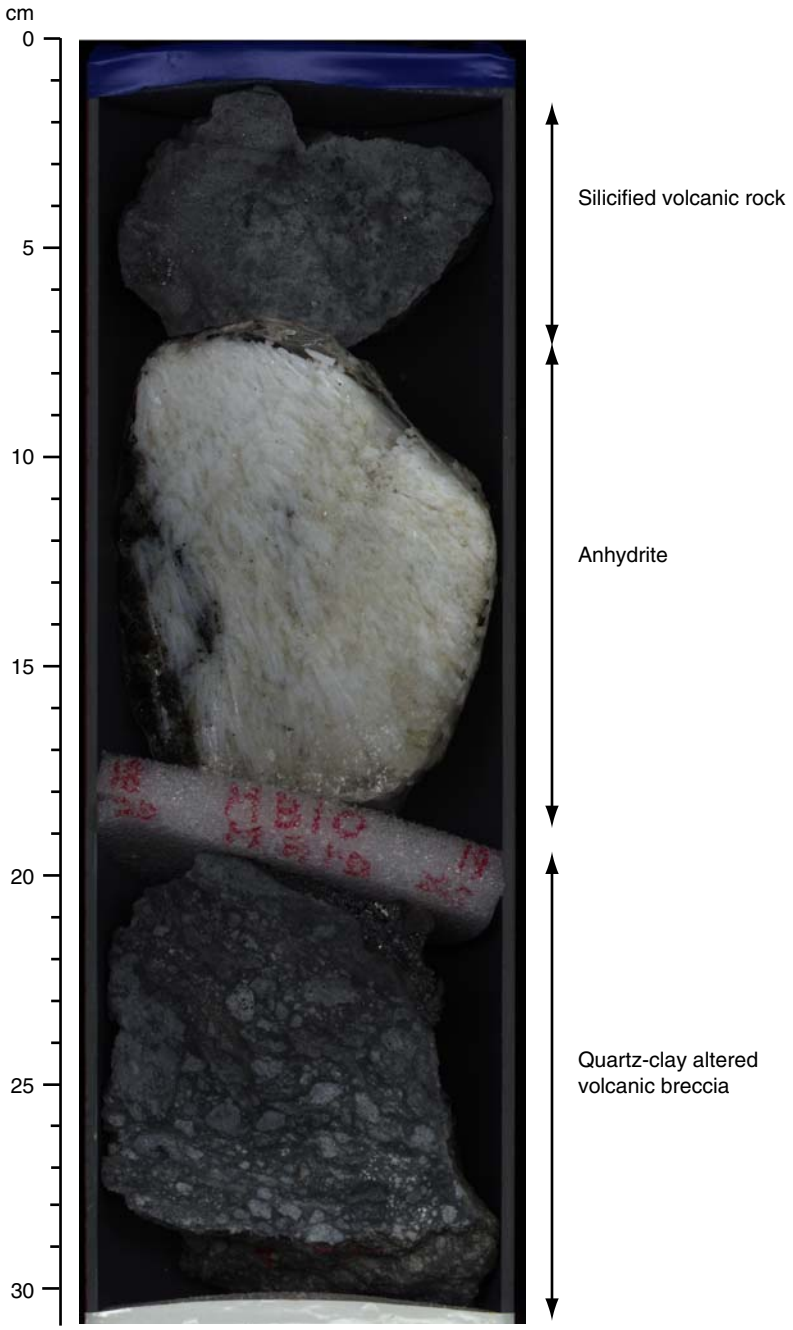

Figure F7. Core photographs showing veining in quartz-chlorite altered volcanic rock. **A.** Network of quartz-chlorite pyrite veins (interval 331-C0016B-3L-1, 3–19 cm). **B.** Quartz-chlorite-pyrite vein (indicated by white outline) cut by later anastomosing pyrite-anhydrite vein network (interval 331-C0016B-3L-CC, 0–13 cm).

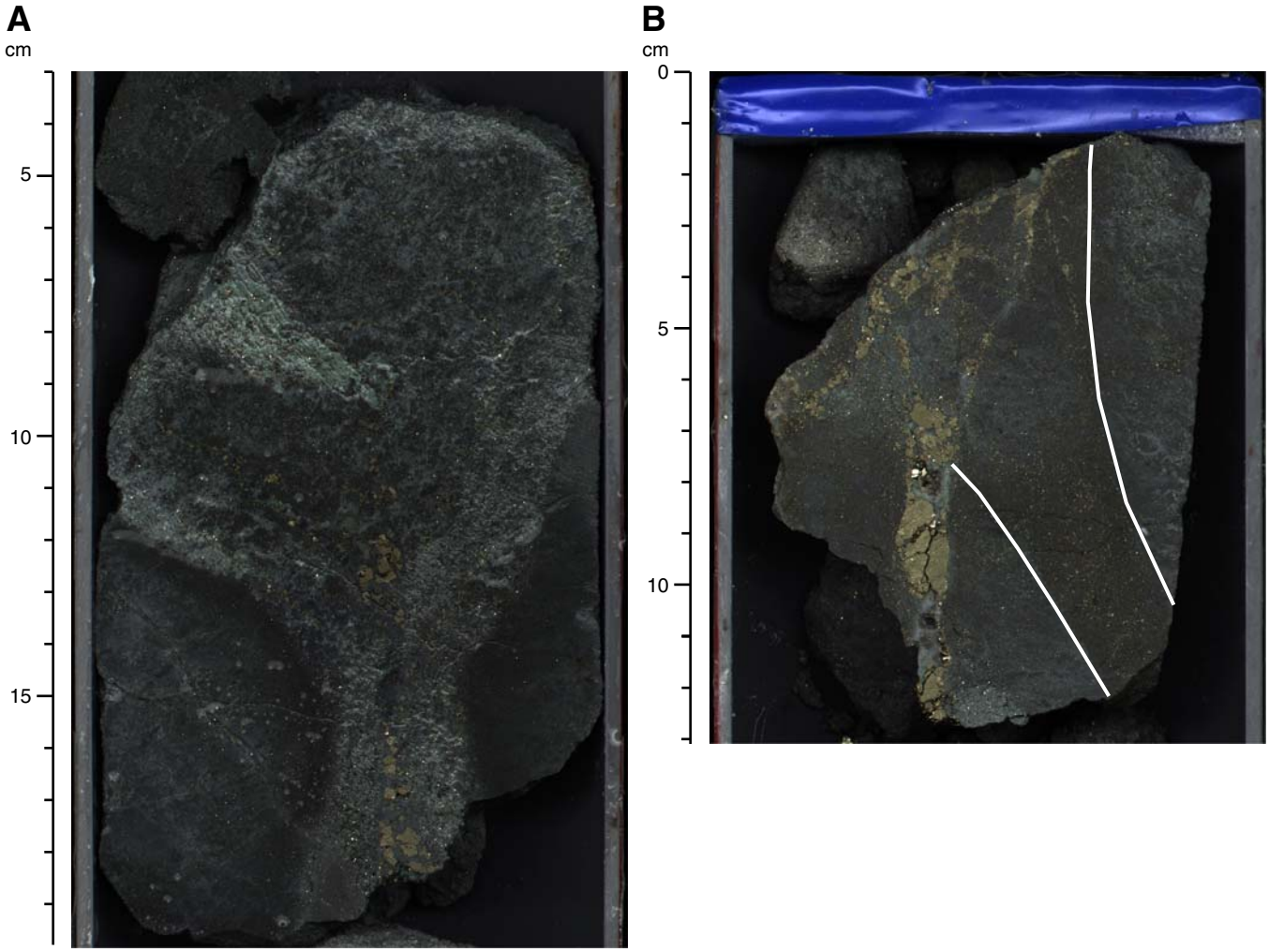

Figure F8. Plot of discrete measurements of bulk density, grain density, and GRA-derived bulk density from the multisensor core logger for whole-round samples (MSCL-W), Site C0016. GRA-derived bulk density values <0 g/cm^3 are omitted for clarity.

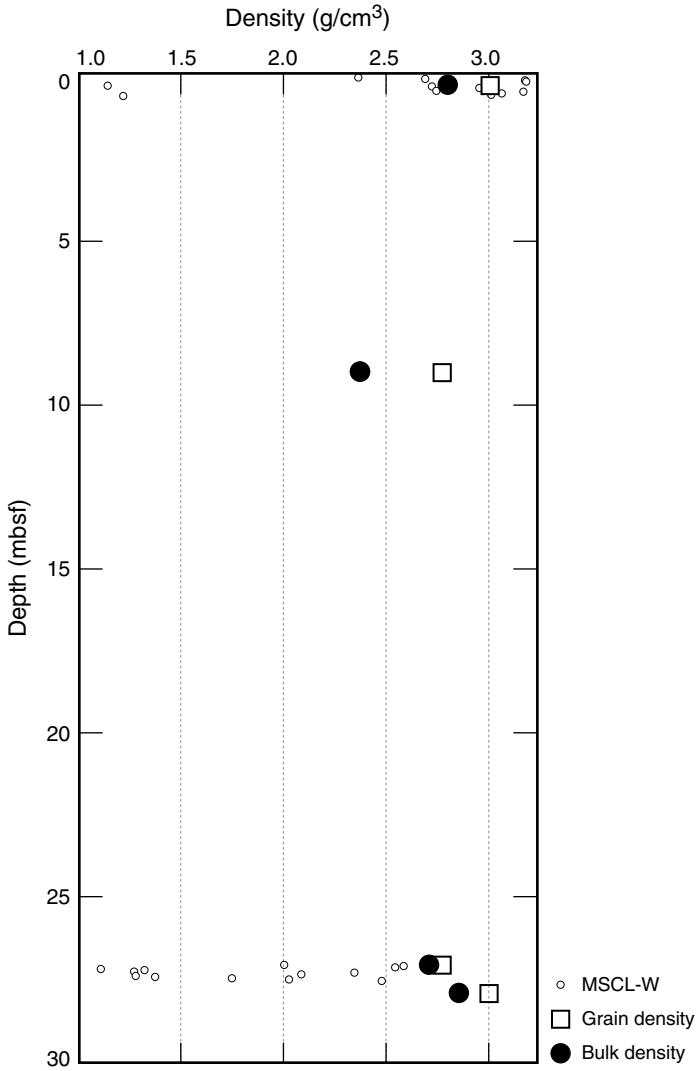

Figure F9. Plot of porosity calculated from discrete MAD measurements, Site C0016.

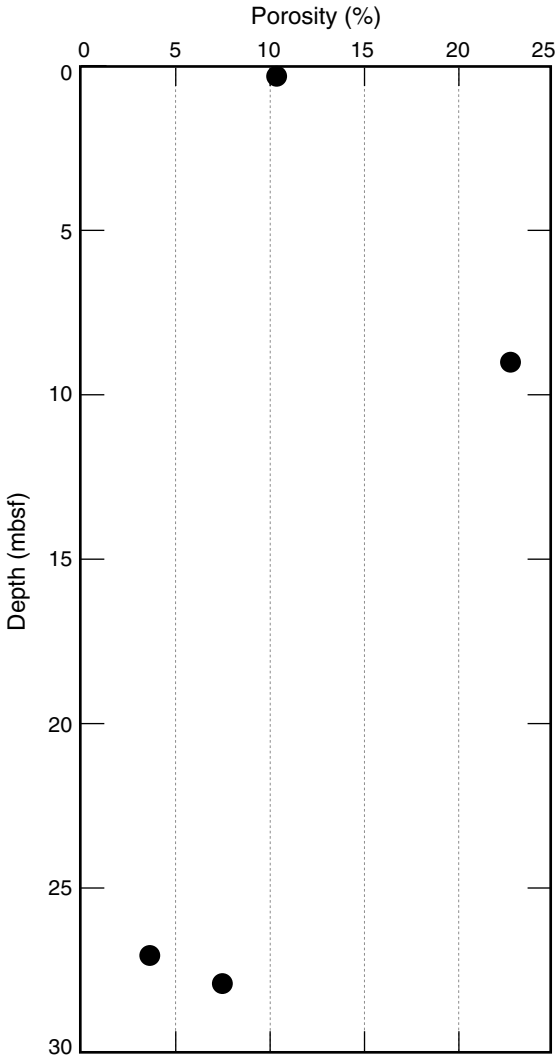

Figure F10. Plot of discrete measurements of *P*-wave velocity, Site C0016.

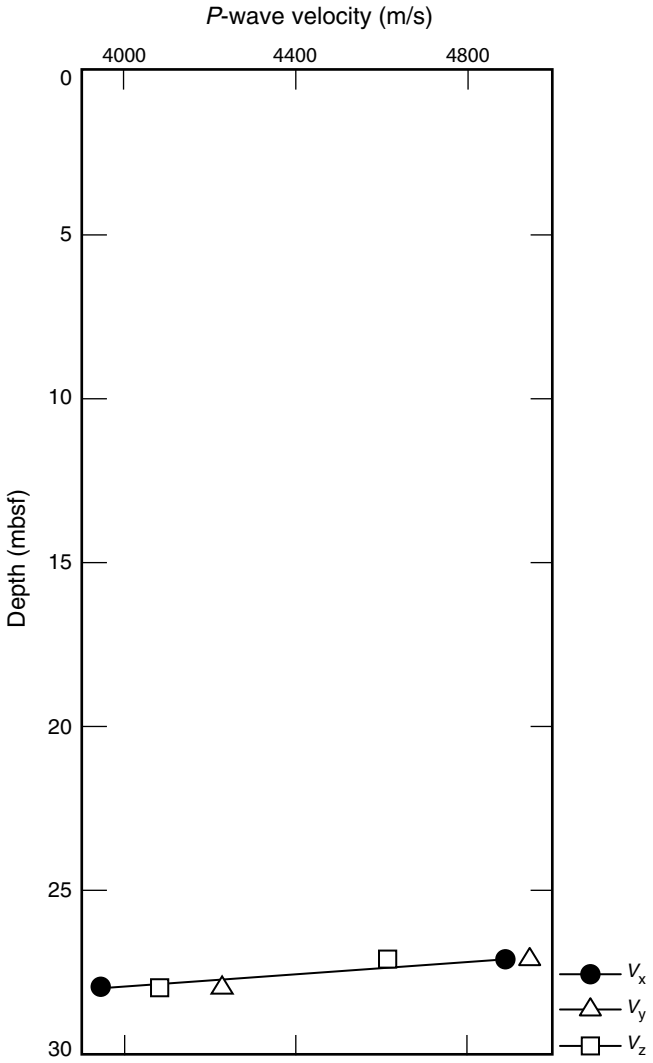

Figure F11. Plot of thermal conductivity, Site C0016.

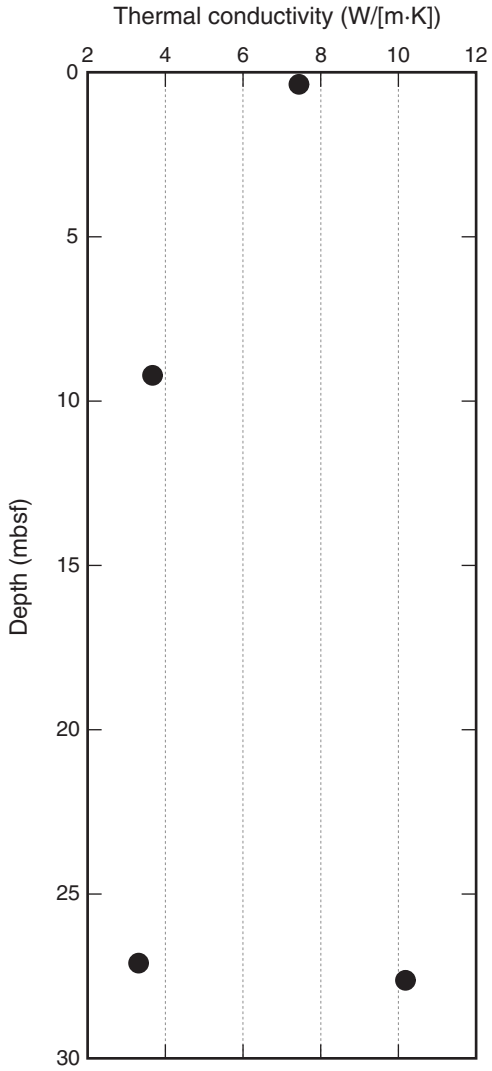

Figure F12. Plot of MSCL-W-derived electrical resistivity, Site C0016.

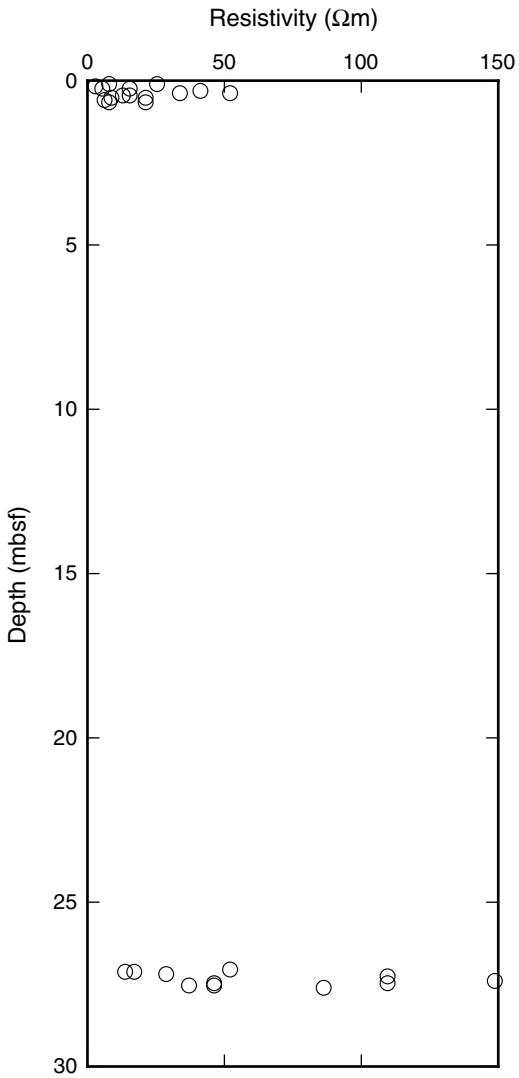

Table T1. Coring summary, Site C0016.

Site C0016
Time on site (h): 79

Hole C0016A
Latitude: 27°47.4548′N
Longitude: 126°53.8034′E
Time on hole (h): 11.5 (0001 h, September 26–1130 h, September 26)
Seafloor depth (m DRF): 1010.5
Distance between rig floor and sea level (m): 28.5
Water depth (mbsl): 982
Total depth (m DRF): 1028.5
Total penetration (mbsf): 18
Total length of cored section (m): 18
Total core recovered (m): 0
Core recovery: 0
Total number of cores: 0

Hole C0016B
Latitude: 27°47.4538′N
Longitude: 126°53.7860′E
Time on hole (h): 67 (2055 h, September 30–1535 h, October 3)
Seafloor depth (m DRF): 1023.5
Distance between rig floor and sea level (m): 28.5
Water depth (mbsl): 995
Total depth (m DRF): 1072.2
Total penetration (mbsf): 44.9
Total length of cored section (m): 44.9
Total core recovered (m): 1.74
Core recovery: 3.9
Total number of cores: 3

Core	Date (2010)	Local time (h)	Depth DRF (m) Top	Depth DRF (m) Bottom	Depth (mbsf) Top	Depth (mbsf) Bottom	Advanced (m)	Recovered (m)	Recovery (%)
331-C0016A-									
1L	26 Sep	0430	1010.5	1028.5	0	18	18	0	0
331-C0016B-									
1L	30 Sep	2055	1027.3	1036.3	0	9	9	0.71	7.9
2L	1 Oct	2035	1036.3	1054.3	9	27	18	0.31	1.7
3L	2 Oct	1525	1054.3	1072.2	27	44.9	17.9	0.72	4

DRF = drilling depth below rig floor. L = BHI.

Table T2. Interpreted results of X-ray diffraction (XRD) analyses of samples, Site C0016.

Sample number	Core, section, interval (cm)	Lithology	Subsampled for	Result
	331-C0016B-			
36435	1L-1, 18–20	Clastic textured "black ore" massive sulfide	Routine chemistry	Sphalerite/wurtzite, quartz, anhydrite, pyrite, galena, muscovite (trace)
36438	1L-CC, 12–14	Silicified volcanic rock with disseminated sulfide	Routine chemistry	Quartz, galena, pyrite, sphalerite/wurtzite, anhydrite, muscovite (trace), carlinite (Ti_2S) ???
36526	2L-CC, 4–6	Silicified volcanic breccia	XRD only—mineralogy	Quartz, pyrite, sphalerite/wurtzite, muscovite (trace)
36527	2L-CC, 9–10	Anhydrite	Routine chemistry	Anhydrite
36529	2L-CC, 28–31	Silicified volcanic breccia	XRD only—mineralogy	Quartz, pyrite, anhydrite (trace), muscovite (trace)
36556	3L-CC, 30–32	Dark green chloritic volcanic	XRD only—mineralogy	Quartz, pyrite, chlorite, acanthite (Ag_2S) ???

Phases listed in approximate order of decreasing abundance.

Table T3. Concentrations of hydrocarbons observed in safety gas vials, Hole C0016B.

Hole, core, section, interval (cm)	Depth (mbsf)	CH_4 in headspace (ppm)	C_2H_6 in headspace (ppm)	C_3H_8 in headspace (ppm)	Butane, ethylene, and/or propylene (Y or N)	Sediment mass (g)	CH_4 in pore water (μM)	C_2H_6 in pore water (μM)
331-C0016B-3L-1, 0	27.00	1.8	BD	BD	Y	3.0	310.5	NA

BD = below detection, NA = not applicable.

Table T4. Concentrations of H_2 and CH_4 in science gas, Hole C0016B.

Hole, core, section, interval (cm)	Depth (mbsf)	H_2 in headspace (ppm)	CH_4 in headspace (ppm)	Sample mass (g)	H_2 in pore water (nM)	CH_4 in pore water (μM)
331-C0016B-3L-1, 0–4	27.00	34.6	9.2	25.44	324,244.5	86.1

Table T5. Carbon, nitrogen, and sulfur, Site C0016.

Core, section, interval (cm)	Depth (mbsf)	IC (wt%)	$CaCO_3$ (wt%)	TN (wt%)	TC (wt%)	TS (wt%)	TOC (wt%)	TOC/TN
331-C0016B-								
1L-1, 18.0–20.0	0.27	0.0005	0.0042	BD	0.022	21.2	0.022	NA
1L-CC, 12.0–14.0	0.76	BD	BD	BD	0.009	7.7	0.009	NA
2L-CC, 9.0–10.0	9.09	0.0066	0.055	BD	0.014	23.2	0.007	NA

IC = inorganic carbon, TN = total nitrogen, TC = total carbon, TS = total sulfur, TOC = total organic carbon. BD = below detection, NA = not applicable.

Table T6. Perfluorocarbon tracer (PFT) concentrations in mud adhered on rock surface, Hole C0016B.

Core, section	PFT in test vial gas phase (ppm)	Sample weight in test vial (g)	PFT per g sample (ppm)
331-C0016B-			
2L-CC	9.76E–02	0.09	1.08E+00
3L-1	7.08E–01	0.53	1.34E+00